

## **FRAGILITY CURVES FOR ROCKING MASONRY FAÇADES OF CHURCHES: A SENSITIVITY STUDY OF VULNERABILITY PARAMETERS**

**L.U. Argiento<sup>1</sup>, C. Casapulla<sup>2</sup> and F. Ceroni<sup>1</sup>**

<sup>1</sup> Department of Engineering, University of Napoli 'Parthenope', Napoli, Italy  
Centro Direzionale is.C4, Napoli 80143, Italy  
[archargiento@libero.it](mailto:archargiento@libero.it), [francesca.ceroni@uniparthenope.it](mailto:francesca.ceroni@uniparthenope.it)

<sup>2</sup> Department of Structures for Engineering and Architecture  
Via Forno Vecchio 36, Napoli 80134, Italy  
[casaccla@unina.it](mailto:casaccla@unina.it)

---

### **Abstract**

*Out-of-plane failure of façades is one of the most distinctive local mechanisms in masonry churches recognizable in the aftermath of a seismic event. The purpose of this paper is to derive large-scale fragility curves for masonry church façades using incremental static analysis, and to assess the influence of some parameters on their vulnerability. According to the displacement-based approach, pushover analysis is carried out considering both the geometric nonlinearities and the stabilizing contribution of frictional resistances exerted by the church sidewalls. The seismic demand is derived using acceleration-displacement response spectra (ADRS) for different limit states, obtained according to the Italian seismic code. The analyses are addressed with reference to a large sample of masonry churches generated starting from the geometric parameters of a reduced sample of churches hit by the seismic event of 21<sup>st</sup> August 2017 in the Ischia Island (Italy). Several geometric aleatory variables, i.e. the length, the height and the thickness of the façade, are treated by means of the Monte Carlo simulation (MCS) to generate a numerical sample of 400 facades. Considering two limit states for rocking (moderate and severe motion), fragility curves are derived for these facades subjected to the same single ground motion scaled at different values of PGA, using incremental static analysis (ISA) and multiple stripe analysis (MSA). Finally, on the same sample of 400 facades, the sensitivity of the fragility curves to the friction coefficient, the length of masonry units and the position of the façade mass center is investigated.*

**Keywords:** Rocking, Incremental Static Analysis, Frictional Resistances, Monte Carlo Simulation, Fragility Curves, Multiple Stripe Analysis.

---

## 1 INTRODUCTION

The damage assessment of masonry churches after the recent seismic events occurred in Italy has highlighted the great vulnerability of these types of structures. The Italian territory is characterized by an architectural heritage of great value which needs to be preserved. These aspects lead to a growing interest of the scientific community into assessing the seismic risk of existing masonry churches [1-4]. The high vulnerability of churches is mainly due to some peculiar structural features, i.e. slender walls with large opening, thin long span vaults, trusting horizontal structures, etc. These peculiarities often make it possible the activation of local failure mechanisms and evidence the importance to assess the church as a set of macro-elements. In particular, the out-of-plane failure of the façade has been frequently observed in masonry churches in the aftermath of a seismic event and is, indeed, one of the most representative local mechanisms for a church. In fact, the rocking of façades is the most recurring mechanism in terms of percentage concerning the possible and activated mechanisms, as observed in recent earthquakes [1, 5]. Recently, different analytical and numerical approaches were developed to analyze the seismic response of rocking façades [6-9], also restrained by dissipative devices [10, 11] or by optimal economic and environmental retrofitting solutions [12].

In this paper, the façades are modeled as rigid blocks and their out-of-plane response is addressed through the nonlinear kinematic approach of limit analysis. In particular, an advanced macro-block model accounting for frictional resistances is herein adopted to consider the effect of the interlocking of the façades with the sidewalls [6]. The seismic input is represented in terms of over-damped elastic acceleration-displacement response spectra (ADRS) derived from the analytical functions of the hazard parameters provided by the Commentary to the Italian seismic code, namely CNTC19 [13]. A direct relation is defined between the peak ground acceleration (PGA) associated with a scaled spectral shape and the displacement demand for the rocking mechanism of each façade wall. This relation is developed through the construction of incremental static analysis (ISA) curves, obtained according to the procedure suggested by PERPETUATE Guidelines [7].

The analyses are carried out on a large sample of masonry church façades (400) obtained starting from the geometric parameters of 14 single-nave churches hit by the seismic event of 21st August 2017 in the Ischia Island (Italy). The capacity curves for the 14 façades were already obtained in a previous work [14] according to the displacement-based approach, and their seismic assessment was carried out as well. The goal of this paper is to expand this small sample into an extensive database in order to implement fragility curves with a large-scale approach. In fact, assuming probabilistic distributions of the main geometric parameters detected in the 14 facades, the numerical database is generated through a Monte Carlo simulation (MCS). Analytical fragility curves are, thus, obtained using ISA and multiple stripe analysis (MSA) for discrete intervals of PGA, and with reference to the engineering demand parameters (EDPs) for each of the two limit states (moderate and severe rocking). Finally, on the same sample of 400 facades and for both limit states, the sensitivity of the fragility curves to the friction coefficient, the length of masonry units and the position of the façade mass center is investigated.

The original contribution of the paper consists in highlighting the influence of the geometric parameters of the façade and of its interlocking restraints with sidewalls on the church façade vulnerability to out-of-plane mechanisms with a large-scale approach. The results of this study may be a great support in assessing the reduction of seismic vulnerability together with the use of earthquake-resistant devices [15, 16].

## 2 DATABASE DESCRIPTION AND CATEGORIZATION OF ALEATORY VARIABLES

In this section, the characteristics of the Ischia churches and the categorization of aleatory variables adopted to define the numerical database are presented in order to build the fragility curves in the following sections.

### 2.1 Nonlinear kinematic approach

Using nonlinear kinematic analysis, the capacity curves for the façades are obtained according to the displacement-based approach [17]. Adopting the macro-block model developed by Casapulla and Argiento [6], the façade is assumed rotating around its external bottom edge, while the units along the two vertical crack lines exhibit a rocking-sliding motion with a clear prevalence of sliding. The frictional resistances developed along the vertical crack lines, which separate the façade wall from the sidewalls, exert a restraining action against the rocking motion. The model is used to perform the pushover curves predicting the capacity of the selected façades in terms of the horizontal action activating the mechanism and its evolution at large displacements [14]. These curves are obtained considering a nonlinear reduction of the frictional resistances due to the progressive detachment of the rocking façade from the sidewalls [6].

The procedure was firstly applied to 14 selected churches [14] hit by the seismic event of 21<sup>st</sup> August 2017 and located in five different villages of the Ischia Island: Barano d'Ischia, Casamicciola Terme, Forio, Lacco Ameno and Serrara Fontana.

Masonry block walls with regular units and staggering are considered (single-leaf walls arranged in a running bond pattern). As close to the real walls, the single unit is assumed with height equal to 150 mm and length as a variable parameter, while its thickness is always assumed coincident with that of the walls (Fig. 1a).

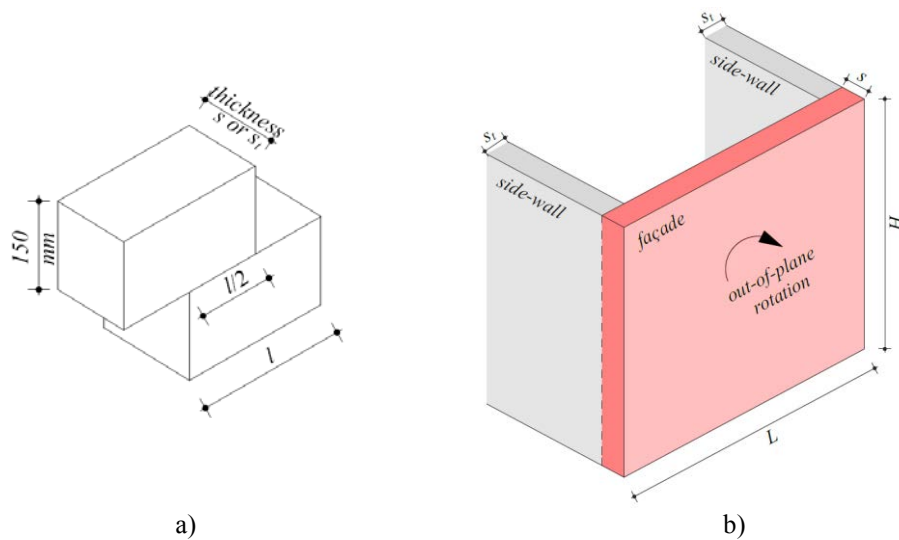


Figure 1: Geometric parameters of a) the block and b) the façade.

The specific weight of masonry is considered equal to  $18 \text{ kN/m}^3$ , indicative of the Ischia tuff. Table 1 reports the real dimensions of the 14 façades (see also Fig. 1b for the symbols) together with the normalized values of their slenderness ratios in terms of lower and upper bounds and mean values. In particular,  $\lambda_l = L/s$  is considered the horizontal slenderness of the façade, while  $\lambda_f = H/s$  and  $\lambda_s = H/s_t$  represent the vertical slenderness of the façade and of the

sidewalls, respectively. It is worth highlighting that the standard deviation of  $L$  in the last column has been reduced from 5 to 2 in order to avoid unrealistic hypotheses of the façade length.

Parameter	Lower bound	Upper bound	Mean	St. Dev.
$s$	<b>0.50</b>	<b>1.05</b>	<b>0.80</b>	<b>0.15</b>
$H$	7.20	14.00	10.08	2.10
$L$	6.50	26.00	10.73	2.00
$s_t$	0.50	0.90	0.76	0.12
$\lambda_f$	<b>9.50</b>	<b>16.47</b>	<b>12.63</b>	<b>1.71</b>
$\lambda_s$	<b>9.50</b>	<b>20.00</b>	<b>13.40</b>	<b>2.69</b>
$\lambda_l$	<b>8.35</b>	<b>27.37</b>	<b>13.20</b>	<b>2.29</b>

Table 1: Categorization of aleatory variables.

In order to compare the seismic capacity and demand for the following checks, it is necessary to define the capacity curve, i.e., the acceleration vs. displacement curve. Fig. 2 shows the typical capacity curves related to both the ‘free’ (dotted line) and ‘restrained’ (continuous line) rocking conditions for the façade of one of the Ischia churches. It clearly emerges that the frictional resistances strongly increase the acceleration that activates the mechanism, and the trend of the capacity curves along the evolution of the mechanism is strictly related to the variation of the frictional resistances. In the case of ‘restrained’ condition, the first branch of the capacity curve is linearly decreasing as it corresponds to the constant contribution of frictional resistances. Then, the curve has a stepwise linear decreasing trend due to the progressive loss of contact along the blocks starting from the top of the interlocked walls. When all the frictional resistances become null, the capacity curve for the restrained façade coincides with that corresponding to the free rocking condition.

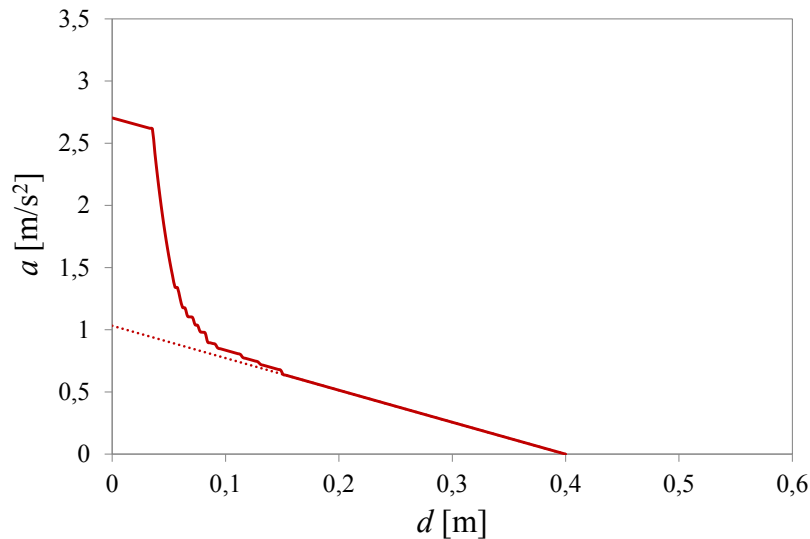


Figure 2: Capacity curves related to the free (dotted line) and restrained (continuous line) rocking conditions for one of the 14 selected façades of the Ischia churches.

## 2.2 Database generation

The seismic behavior of the church façades is largely affected by the variability of their geometric dimensions, which can be considered as aleatory uncertainties. These are related to

the randomness of a certain phenomenon and are classified as irreducible uncertainty referring to a property of the system associated with more variability [18].

The aleatory variables herein involved are the dimensions related to the slenderness values of both the facade and the sidewalls (Table 1) and are treated by the MCS [19]. Fig. 3 shows the steps adopted with the aim to generate realistic cases of façades. In particular, starting from the thickness of a façade, the geometric parameters are linked to each other through defined values of the three reference values of slenderness. A total of 400 simulations are assumed being enough to reach a good reliability of results.

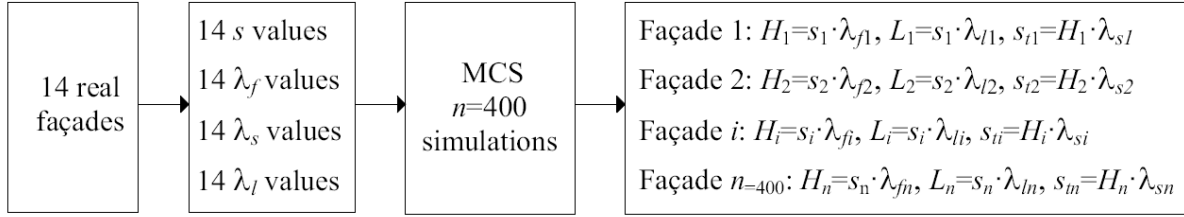


Figure 3: Steps from 14 real façades to the generation of 400 façades through the MCS.

Fig. 4 shows the frequency histograms for the geometric values used in the analyses relating to the thickness ( $s$ ), height ( $H$ ) and length ( $L$ ) of the façade together with thickness of sidewalls ( $s_t$ ), where  $H$ ,  $L$  and  $s_t$  are derived through the slenderness values. It can be noted that the use of the MCS leads to a distribution of the geometric parameters consistent with the real observed ones (see the lower and upper bounds and the mean values of Table 1), confirming the effectiveness of the choices.

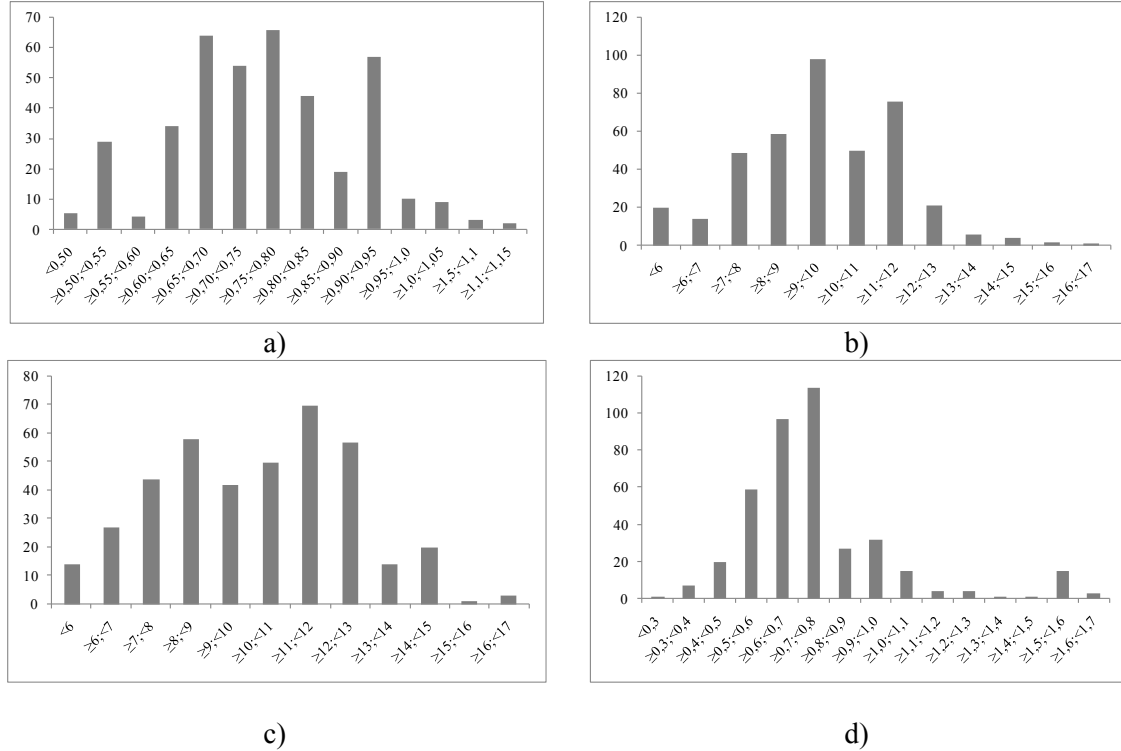


Figure 4: Distribution of the sample of 400 churches with reference to a)  $s$ , b)  $H$ , c)  $L$  and d)  $s_t$ .

### 3 SEISMIC ASSESSMENT: DESCRIPTION OF THE APPROACH, SEISMIC INPUT AND EDP

#### 3.1 Definition of the limit states for rocking

For the correct evaluation of the fragility curves, an appropriate EDP is necessary for its association with damage states. To this aim, the two ultimate limit states indicated by the CNTC19 [13] are here considered for the seismic assessment of the out-of-plane failure of the generated façades. LS1 (moderate rocking), representative of the life-safety limit state, occurs when the displacement of the control point attains the value  $d_{LS1} = 0.4 d_0$ , where  $d_0$  corresponds to the loss of static equilibrium (e.g., when  $d_0$  becomes equal to the half-thickness of the façade wall in the unrestrained condition). On the other hand, LS2 (severe rocking) is associated with  $d_{LS2} = 0.6 d_0$ , which is representative of the collapse limit state. Fig. 5 shows a scheme summarizing the matching among limit state/rocking phase/capacity/demand for each limit state (LS0, LS1 and LS2), where LS0 corresponds to the activation of the motion.

Once defined the reference displacement capacities for LS1 and LS2, the procedure requires deriving the corresponding values of the equivalent secant periods  $T$  through the following relations:

$$T_{LS1} = 1.68\pi \sqrt{\frac{d_{LS1}}{a(d_{LS1})}} \quad T_{LS2} = 1.58\pi \sqrt{\frac{d_{LS2}}{a(d_{LS2})}} \quad (1)$$

where  $a(d_{LS1})$  and  $a(d_{LS2})$  are the accelerations corresponding to the reference displacements on the capacity curve. The displacement demand for a specific limit state and for each façade is, thus, obtained from the intersection of the ADRS provided by the code and the line starting from the origin of the axes and having an inclination corresponding to the equivalent period given by Eq. (1). Following the indications of CNTC19 [13], the assumed values of the damping ratio of the over-damped ADRS are 8% and 10% for LS1 and LS2, respectively.

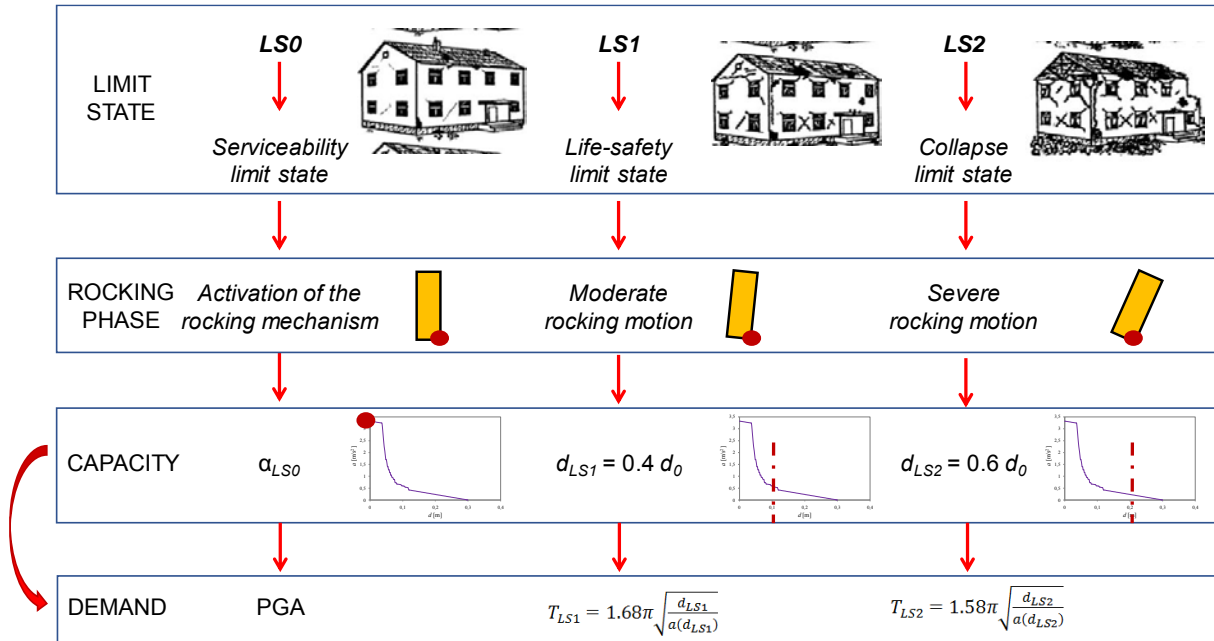


Figure 5: Correlation of each limit state (LS0, LS1 and LS2) with the rocking phase, capacity and demand.

### 3.2 Definition of the seismic input

According to the capacity spectrum method (CSM) indicated by the current Italian seismic code [13, 20], the seismic demand is derived from over-damped elastic acceleration-displacement response spectra (ADRS), based on analytical functions of hazard parameters. For the site-specific earthquake ground motion parameters, a soil type B (deposits of very dense sand, gravel, or very stiff clay) is assumed, and the soil factor  $S$  is fixed equal to 1.2 accounting for topographic and stratigraphic conditions. Table 2 reports the seismic demand parameters with reference to the design spectrum for the site of Casamicciola (Ischia).

Limit state	$a_g$ [g]	$S$	$F_0$	$T_c^*$	$\eta$	$T_r$ [years]
LS1	0.152	1.200	2.285	0.325	0.877	475
LS2	0.200	1.200	2.333	0.325	0.816	975

Table 2: Hazard parameters related to LS1 and LS2, with reference to the design spectrum of Casamicciola (Ischia) according to [13, 20].

In [14], the capacity curves for the 14 facades of the Ischia churches were built according to the procedure described in section 2.1 and the safety checks related to LS0, LS1 and LS2 for the expected seismic action in the site were carried out using the hazard parameters listed in Table 2. All checks were satisfied, with higher values of the ratio capacity/demand when frictional resistances were taken into account.

In the following, the same procedure is applied to the extended database of 400 facades, considering the variability of both the geometric parameters and the seismic input in order to build large-scale fragility curves for LS1 and LS2. In particular, ISA are developed to take into account the variability of the seismic intensity and MSA is used to build the fragility curves.

### 3.3 Assessment of the displacement demand via ISA

As regards the relation between the peak ground acceleration associated with a scaled spectral shape and the displacement demand, ISA curves are developed according to the procedure suggested by [13]. For this purpose, the ADRS related to LS1 and LS2 are normalized with respect to their PGA and the following expression is adopted to define the scale factor IM, representing the value of  $PGA/g$  that provides a displacement demand  $d^*$  equal to the capacity  $d$ :

$$IM(d^*) = \frac{d^*}{S_{d1}(T^*) S} = \frac{PGA}{g} \quad (2)$$

where  $S_{d1}(T^*) = S_d(T^*)/(PGA/g)$  is the displacement provided by the normalized over-damped ADRS.

Figure 6 reports the ISA curves obtained for one church of the database, considered as an example. These curves, derived from the scaled code spectra for both LS1 (Fig. 6a) and LS2 (Fig. 6b), represent the relation between the displacement demand and IM by changing the secant periods.

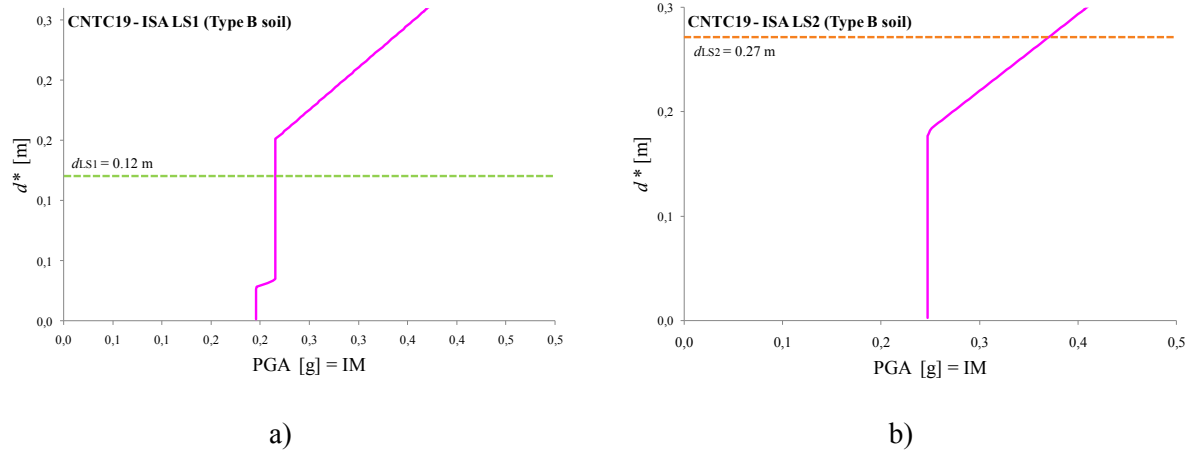


Figure 6: ISA curves derived from code spectra related to a) LS1 and b) LS2 for one of the Ischia churches.

The curves obtained by ISA can represent an interesting tool to express the results of the seismic analysis in terms of PGA, being this intensity measure largely used in the field of the seismic hazard assessment. In fact, the PGA value that activates a specific limit-state displacement can be assumed as the capacity related to the assumed spectral shape of the seismic input and, then, it can be compared with the PGA representing the demand for the same limit state.

As shown in Figs. 6a and 6b, the intersections between the ISA curves and the displacement demands  $d$  equating the displacement capacity (i.e.  $d_{LS1} = 0.12$  m and  $d_{LS2} = 0.27$  m) allow defining the capacities in terms of PGA providing LS1 and LS2 for the façade (i.e.  $PGA_{dLS1} = 0.22$  g and  $PGA_{dLS2} = 0.37$  g), respectively.

### 3.4 Definition of fragility curves via MSA and likelihood function

The procedure for calculating the exceeding probability of a specific damage state is based on the application of MSA [18, 21]. In particular, the ratio between each PGA/g step (0.05, 0.15, 0.25, 0.40, 0.65) and the previously calculated capacities  $PGA_{dLS1}$  or  $PGA_{dLS2}$  for each façade is defined as the EDP for each LS1 or LS2 and for each scaled spectrum obtained by the design one expected for the site of Casamicciola. All these EDPs, representing the demand/capacity ratios, are plotted versus the PGA ranges for both limit states in Figs. 7a and 7b.

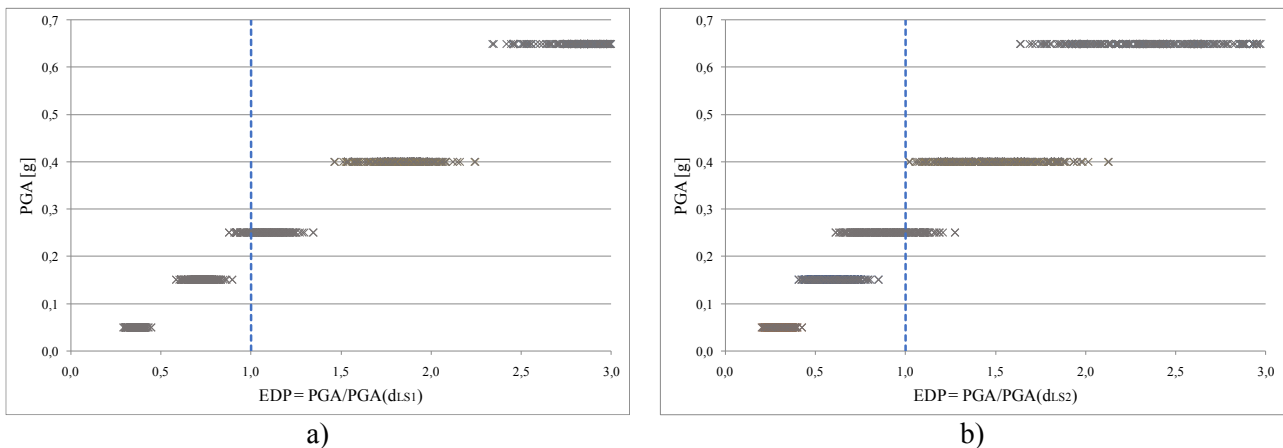


Figure 7: MSA based on the code spectra and related to the 400 facades for a) LS1 and b) LS2.



The distributions of these ratios for the 400 façades have a ‘stripe’ shape for each PGA and allow to simply check if a limit state is attained or not by comparing the EDP with the unity value.

Then, the probability of occurrence of a given limit state, only LS1 or LS2 for the case at hand, is computed by counting how many times for a given PGA, the EDP is greater than 1. This allows plotting discrete fragility curves that can be fitted by analytical lognormal distributions, as widely adopted in the literature [22]. The probability that an arbitrary PGA value causing a given limit state,  $LS_i$ , is attained, i.e. the fragility function, can be defined through the following well-known probability density function:

$$P(LS_i|PGA) = \Phi\left(\frac{\ln(\frac{x}{\theta})}{\beta}\right) \quad (3)$$

where  $\Phi$  denotes the standard normal cumulative distribution function (CDF) of the variable  $\ln(x/\theta)$ , being, usually,  $x$  equal to the PGA,  $\theta$  is the median value of the fragility function for a given  $LS_i$  (i.e., the PGA value corresponding to 50% probability of attaining  $LS_i$ ) and  $\beta$  is the standard deviation of  $\ln(PGA)$ , representing the slope of the fragility curves in correspondence with  $\theta$ . The estimation of  $\theta$  and  $\beta$  values is done by maximizing the following likelihood function:

$$Likelihood = \prod_{j=1}^m \binom{n_j}{z_j} \Phi\left(\frac{\ln(\frac{x}{\theta})}{\beta}\right)^{z_j} \left(1 - \Phi\left(\frac{\ln(\frac{x}{\theta})}{\beta}\right)\right)^{n_j - z_j} \quad (4)$$

where  $z_j$  is the number of cases with  $EDP \geq 1$ , i.e. a given  $LS_i$  is exceeded,  $n_j$  is the total case belonging to the  $j$ -th range of PGA and considering  $m$  the total number of PGA intervals used for the definition of  $LS_i$ . The best fitting lognormal curve associated with each damage level is, thus, expressed through the  $\theta$  and  $\beta$  values, while the fitting procedure reliability can be evaluated through the likelihood value.

Finally, Fig. 8 shows the fragility curves for the rocking masonry façades of the 400 churches obtained for LS1 and LS2, together with probability of attaining the related limit states derived by MSA.

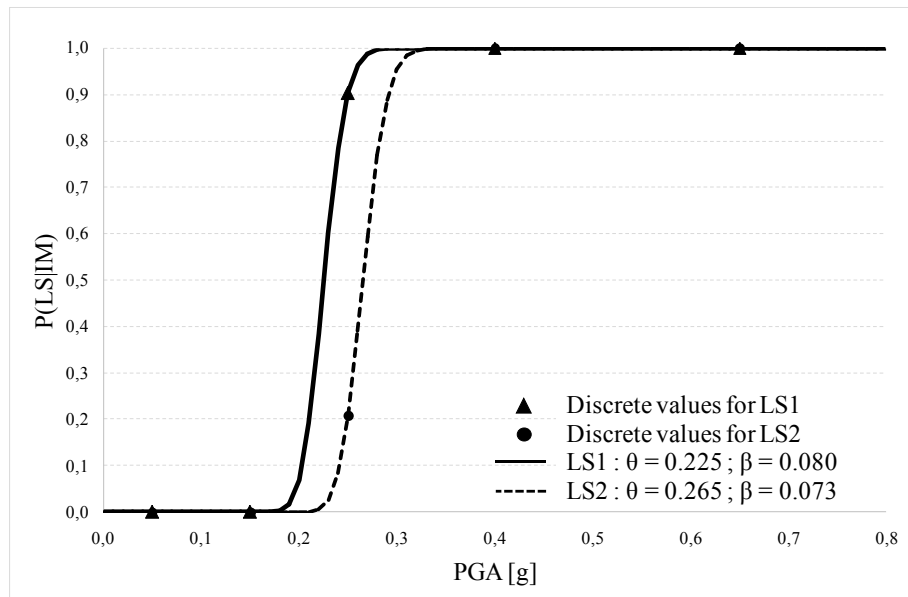


Figure 8: Fragility curves for the sample of 400 churches for LS1 and LS2.

#### 4 FRAGILITY ANALYSIS: SENSITIVITY TO VULNERABILITY PARAMETERS

The development of fragility curves allows to analyze the sensitivity of each limit state condition for rocking façades to vulnerability parameters. This tool is extremely useful bearing in mind that each fragility curve summarizes the behavior of 400 façades. Table 3 reports the chosen ranges of the parameters adopted for the sensitivity analysis: the unit length, the friction coefficient and the center of the façade mass. The bolded numbers represent the values initially assumed in the calculations developed in the previous sections and considered fixed when the other two parameters change. It is worth highlighting that the first two parameters may have large effects on the seismic capacity of the façade since they influence the frictional resistances at its interlocking with sidewalls.

Parameter	Min				Fix				Max
Unit length	0.27	0.30	0.33	0.38	<b>0.43</b>	0.50	0.60	0.75	1.00
Friction coefficient	0.40	0.45	0.50	0.55	<b>0.60</b>	0.65	0.70	0.75	0.80
Center of façade mass	0.30	0.35	0.40	0.45	<b>0.50</b>	0.55	0.60	0.65	0.70

Table 3: Ranges of the values for the vulnerability parameters proposed.

Thus, the procedure explained in sections 3.3 and 3.4 is here repeated again 3 times (one for each parameter assumed variable) for 9 sets (the nine values of each parameter assumed variable) of the 400 facades. Totally, 27 fragility curves are obtained for each *LS*, each curve referring to the 400 façades and variable seismic intensities obtained by scaling the design spectrum expected in the Ischia site according to ISA.

Fig. 9 shows the obtained fragility curves grouped for each single parameter assumed as variable and for limit state (LS1 in the left column, LS2 in the right column).

In particular, Figs. 9a and 9b present the effect of the unit length and evidence a large bundle of curves especially for LS1. These curves are represented by  $\theta$  values included in the ranges from 0.18 to 0.29 and from 0.27 to 0.34 for LS1 and LS2, respectively (Table 4), and make it evident how the unit length plays a relevant role in the vulnerability assessment of rocking façades.

The effect of the friction coefficient  $f$  is shown in Figs. 9c (LS1) and 9d (LS2). It can be observed that the fragility curves for all the façades are almost coincident, with respect to both *LS*. This means that the variation of  $f$  does not significantly impact on the rocking mechanism of the facades. As shown in Table 4, the lower and upper bounds of the  $\theta$  values are included in the range from 0.22 to 0.23 for LS1 and from 0.264 to 0.265 for LS2, respectively.

Finally, Figs. 9e and 9f show the impact of the center of mass position and evidence a medium impact on the rocking mechanism of the façades for LS1, since the  $\theta$  values are included in the ranges from 0.21 to 0.27. As regards LS2, again the bundle is smaller than that for LS1, being included in the range from 0.265 to 0.268.

It is worth highlighting that, in all the sensitivity analyses, LS2 always provides a bundle tighter than LS1. This is due to the fact that, for large displacements, the capacity of the façade in the restrained condition tends to coincide with that in free rocking, and, thus, the influence of the selected vulnerability parameters tend to be negligible [6].

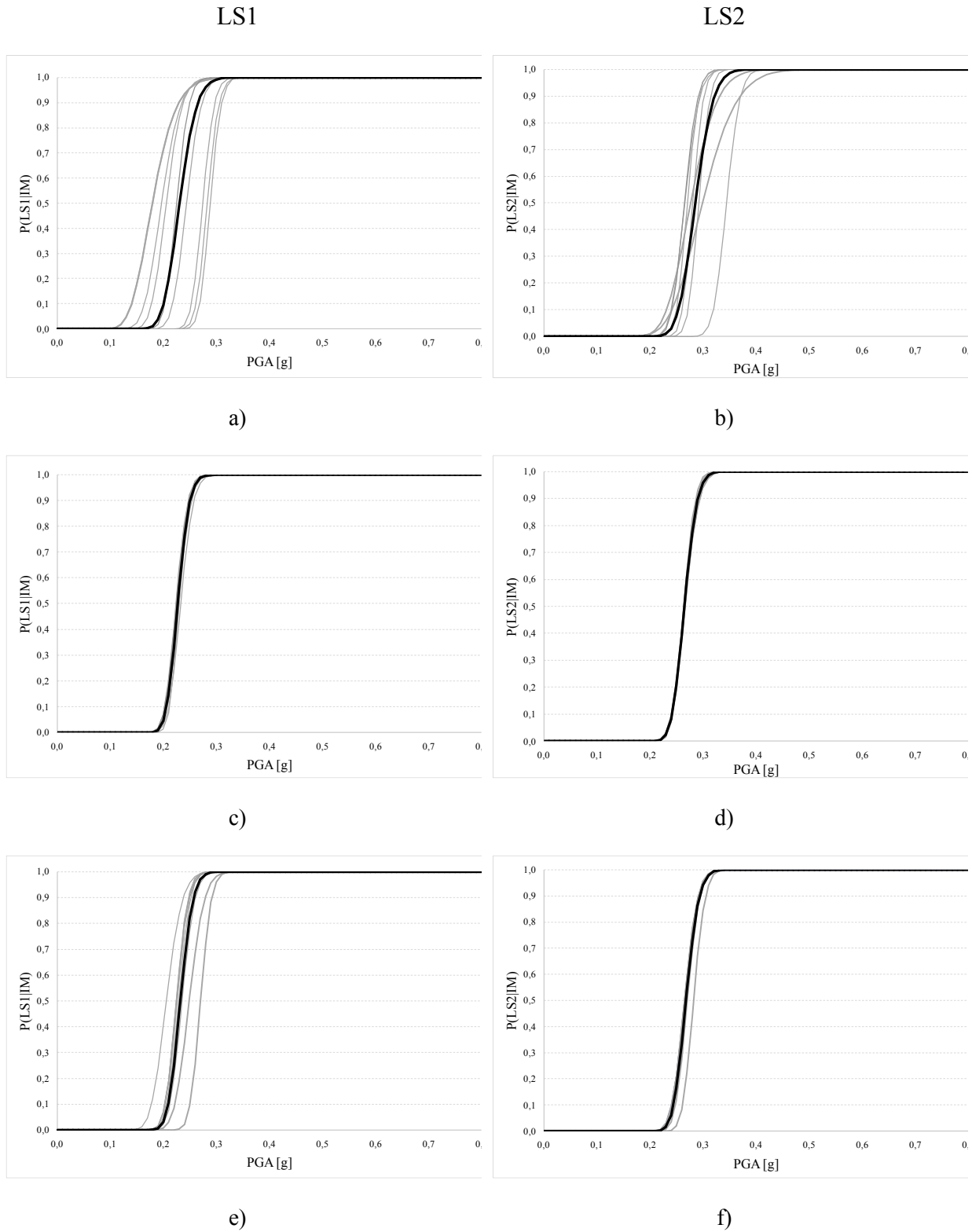


Figure 9: Fragility curves for 400 facades for LS1 (left column) and LS2 (right column) considering the variation of a-b) unit length, c-d) friction coefficient and e-f) center of mass position.

Parameter	Lower bound		Upper bound		Mean	
	$\Theta$ [g]	$\beta$	$\Theta$ [g]	$\beta$	$\Theta$ [g]	$\beta$
<i>LS1</i>						
Length of the block	0.179	0.056	0.289	0.193	0.231	0.109
Friction	0.224	0.063	0.233	0.080	0.227	0.076
Centre of mass	0.206	0.059	0.270	0.113	0.232	0.080
<i>LS2</i>						
Length of the block	0.265	0.056	0.344	0.166	0.286	0.092
Friction	0.264	0.063	0.267	0.078	0.265	0.071
Centre of mass	0.265	0.060	0.283	0.079	0.268	0.071

Table 4: Lower and upper bounds of median ( $\Theta$ ) and standard deviation ( $\beta$ ) for fragility curves with the MCS.

## 5 CONCLUSIONS

Moderate and strong earthquakes generally cause damage to unreinforced masonry churches, especially with the activation of local mechanisms rather than a global behavior. For this reason, the seismic assessment of churches should be mainly based on the vulnerability assessment of the damage associated to possible out-of-plane mechanisms. While fragility curves generally refer to the damage through the estimation of the global index, in this paper the damage was assessed for the single macro-element façade with reference to the simple rocking mechanism.

Starting from the in-situ surveys of 14 actual masonry church façades, aleatory geometric variables were herein treated by the MCS in order to define the geometric dimensions for a large sample of facades. The rocking motion of these façades was analyzed with reference to two limit states, i.e. moderate rocking (LS1) and near collapse (LS2) condition. The capacity curve for each SDOF system was defined through nonlinear kinematic analysis, providing the load factor activating the mechanisms and its evolution till overturning. An advanced macro-block model accounting for frictional resistances was adopted to take into account the interlocking of the façades with the sidewalls. To calculate the seismic demands in terms of PGA for both limit states, ISA curves were carried out by scaling design code spectra and, thanks to the comparisons with the capacity values, MSA were used to calculate the probability of exceeding a given limit state and build the corresponding fragility curve. Each fragility curve is representative of the vulnerability of 400 facades for variable seismic inputs. Successively, the effect of the variation of the unit length, the friction coefficient and the center of mass position was examined on the same numerical database of 400 facades. The sensitivity analysis evidenced that the unit length plays a relevant role on the vulnerability assessment of the masonry church façades. On the other hand, the friction coefficient and the center of mass position have a lower the impact on the rocking mechanism. The fragility functions developed in this paper can be a helpful tool for assessing the influence of geometric and mechanical parameters on a large scale.

Future developments will be focused on the influence on the fragility curves of different seismic inputs (i.e. several spectra different from the one expected in the site), on the assessment of geometric parameters able to identify vulnerability classes of masonry facades, and, finally, on the effects of different strengthening interventions for mitigating the vulnerability of the church façades to rocking.

## ACKNOWLEDGMENTS

This work has been carried out under the financial support of PRIN (projects of significant national interest) 2020, Research project: Smart Monitoring for Safety of Existing Structures and infrastructures (S-MoSES).

## REFERENCES

- [1] F. Ceroni, C. Casapulla, E. Cescatti, V. Follador, A. Prota, F. Da Porto. Damage assessment in single-nave churches and analysis of the most recurring mechanisms after the 2016–2017 central Italy earthquakes. *Bulletin of Earthquake Engineering*, **20**, 8031–8059, 2022.
- [2] C. Canuti, S. Carbonari, A. Dall'Asta, L. Dezi, F. Gara, G. Leoni, M. Morici, E. Petrucci, A. Prota, A. Zona. Post-Earthquake Damage and Vulnerability Assessment of Churches in the Marche Region Struck by the 2016 Central Italy Seismic Sequence. *International Journal of Architectural Heritage*, **15**(7), 1000–1021, 2021.
- [3] G. De Matteis, G. Brando, V. Corlito, E. Criber, M. Guadagnuolo. Seismic vulnerability assessment of churches at regional scale after the 2009 L'Aquila earthquake. *International Journal of Masonry Research and Innovation*, **4**(1–2), 174–196, 2019.
- [4] E. Cescatti, V. Follador, F. Da Porto. Typological analysis and vulnerability curves for masonry churches. *8th International Conference on Computational Methods in Structural Dynamics and Earthquake (COMPDYN 2021)*, Athens, Greece, June 28–30, 2021.
- [5] R. Sisti, L.U. Argiento, C. Casapulla, F. Ceroni, A. Prota, Empirical fragility curves for macro-elements and single mechanisms of churches damaged during the 2016–2017 Central Italy seismic sequence. 19<sup>th</sup> National Conference on “L’Ingegneria Sismica in Italia” (ANIDIS 2022), in *Procedia Structural Integrity*, **44C**, pp. 1380–1387, Turin, Italy, September 11–15, 2022.
- [6] C. Casapulla, A. Maione, L.U. Argiento. Performance-based seismic analysis of rocking masonry façades using non-linear kinematics with frictional resistances: a case study. *International Journal of Architectural Heritage*, **15**(9), 1349–1363, 2021.
- [7] S. Lagomarsino, S. Cattari. PERPETUATE guidelines for seismic performance-based assessment of cultural heritage masonry structures. *Bulletin of Earthquake Engineering*, **13**(1), 13–47, 2015.
- [8] S. Degli Abbatì, S. Cattari, S. Lagomarsino, Validation of displacement-based procedures for rocking assessment of cantilever masonry elements. *Structures*, **33**, 3397–3416, 2021.
- [9] G. de Felice, R. Fugger, F. Gobbin, Overturning of the façade in single-nave churches under seismic loading. *Bulletin of Earthquake Engineering*, **20**, 941–962, 2022.
- [10] O. AlShawa, L. Giresini, C. Casapulla, Comparison of the effects of traditional and innovative tie-rods in reducing the seismic vulnerability of church façades: the case of San Francesco in Mirandola (Italy), 19<sup>th</sup> National Conference on “L’Ingegneria Sismica in Italia” (ANIDIS 2022), in *Procedia Structural Integrity*, **44C**, pp. 1364–1371, Turin, Italy, September 11–15, 2022.

- [11] L. Giresini, F. Taddei, F. Solarino, G. Mueller, P. Croce, Influence of stiffness and damping parameters of passive seismic control devices in one-sided rocking of masonry walls. *Journal of Structural Engineering (ASCE)*, 2021, DOI: 10.1061/(ASCE)ST.1943-541X.0003186.
- [12] L. Giresini, C. Casapulla, P. Croce, Environmental and economic impact of retrofitting techniques to prevent out-of-plane failure modes of unreinforced masonry buildings. *Sustainability*, **13**(20), art. no. 11383, 2021.
- [13] Italian Ministry of Infrastructures and Transports (2019). Circolare n.7 C.S.LL.PP. 2019/01/21. Istruzioni per l'applicazione dell'«Aggiornamento delle “Norme tecniche per le costruzioni”» di cui al decreto ministeriale 17 gennaio 2018. (GU n.35 del 11-02-2019—Suppl. Ordinario n. 5), 2019.
- [14] L.U. Argiento, E. Mousavian, C. Casapulla, F. Ceroni. Pushover analysis of rocking façades in masonry churches: the role of friction and geometry in identifying homogeneous classes of vulnerability. *19<sup>th</sup> ANIDIS Conference, Seismic Engineering in Italy (ANIDIS-ASSISI 2022)*, Turin, Italy, September 11-15, 2022.
- [15] L. Giresini, Effect of dampers on the seismic performance of masonry walls assessed through fragility and demand hazard curves. *Engineering Structures*, **261**, art. no. 114295, 2022, DOI: 10.1016/j.engstruct.2022.114295.
- [16] F. Solarino, L. Giresini, Fragility curves and seismic demand hazard analysis of rocking walls restrained with elasto-plastic ties. *Earthquake Engineering & Structural Dynamics*, **50**(13), 3602-3622, 2021, DOI: 10.1002/eqe.3524.
- [17] S. Lagomarsino. Seismic assessment of rocking masonry structures. *Bulletin of Earthquake Engineering*, **13**, 97-128, 2015.
- [18] M. Nale, F. Minghini, A. Chiozzi, A. Tralli, Fragility functions for local failure mechanisms in unreinforced masonry buildings: a typological study in Ferrara, Italy. *Bulletin of Earthquake Engineering*, **19**, 6049-6079, 2021.
- [19] E. Zio. *The Monte Carlo simulation method for system reliability and risk analysis*. Springer, London, 2013.
- [20] Italian Ministry of Infrastructures and Transports. Decreto n.8 2018/01/17. Aggiornamento delle “Norme tecniche per le costruzioni”. (GU n.42 del 20-02-2018. Serie Generale), 2018.
- [21] J.W. Baker. Trade-offs in ground motion selection techniques for collapse assessment of structures. *Vienna Congress on Recent Advances in Earthquake Engineering and Structural Dynamics (VEESD 2013)*, Vienna, Austria, August 28-30, 2013.
- [22] J. Baker. Efficient analytical fragility function fitting using dynamic structural analysis. *Earthquake Spectra*, **31**(1), 579-599, 2015.